Found: C, 77.09; H, 9.37; N, 3.49.

**$Cp^*_2ScCH_2CH_2C_6H_4$-p-$CF_3$.** $Cp^*_2ScCH_3$ (0.595 g, 1.8 mmol) and p-$CF_3C_6H_4CHCH_2$ (0.32 g, 1.84 mmol) were used as described above to produce $Cp^*_2ScCH_2CH_2C_6H_4$-p-$CF_3$ (0.31 g, 36%), which was isolated by cold filtration. Anal. Calcd for $C_{29}H_{38}F_3Sc$: C, 71.29; H, 7.84. Found: C, 71.11; H, 7.83.

**$Cp^*_2ScCH_2CH_2C_6H_4$-p-$CH_3$.** The same procedure was used as described above, except that p-methylstyrene (0.28 mL, 2.1 mmol) was added to the petroleum ether solution of $[Cp^*_2ScH]_x$ generated from hydrogenation of 0.695 g (2.1 mmol) of $Cp^*_2ScCH_3$. Concentration and cooling of the resulting solution yielded yellow crystals of $Cp^*_2ScCH_2CH_2C_6H_4$-p-$CH_3$ (0.380 g, 42%). Anal. Calcd for $C_{29}H_{41}Sc$: C, 80.15; H, 9.51. Found: C, 79.90; H, 9.46.

**$Cp^*_2ScCH_2CH_2CH_2CH_3$.** A petroleum ether solution of $Cp^*_2ScCH_3$ (0.414 g, 1.3 mmol) was treated with $H_2$ as above. 1-Butene was condensed into the cooled heavy-walled reaction vessel (-196 °C) from a calibrated gas volume. The resulting solution was transferred to a frit assembly. As above, repeated attempts to obtain crystals were unsuccessful. A pale yellow powder (0.165 g, 34% yield) was obtained upon removal of all volatiles. The purity of the compound was checked by $^1H$ NMR (>95%).

**(E)-$Cp^*_2Sc(CH_3)C{=}CH(CH_3)$.** A toluene solution of $Cp^*_2ScCH_3$ (369 mg, 1.12 mmol) was treated with $H_2$ as above. A slight excess of 2-butyne was condensed into the cooled heavy-walled reaction vessel (-196 °C) from a calibrated gas volume. The resulting solution was transferred to a frit and filtered. Repeated attempts to obtain crystals were unsuccessful. An oily orange solid was obtained by removal of volatiles from a pentane solution (149 mg, 36% yield). (E)-$Cp^*_2Sc(CH_3)C{=}CD(CH_3)$ was prepared by an entirely analogous procedure, except that $D_2$ was used in place of $H_2$. $^2H$ and $^1H$ NMR showed that deuterium was located in the vinylic position, with an incorporation of approximately 80%. In addition, some deuterium incorporation into the Cp* rings was observed.[17c]

**Kinetics of β-Hydrogen Elimination of $Cp^*_2ScCH_2CH_2R$ Complexes.** Sealed NMR tubes were prepared and experiments were carried out as described above for the reaction of $Cp^*_2ScCH_3$ with 2-butyne. To determine the dependence of the concentration of 2-butyne on the observed rate constant, a series of experiments were carried out with $Cp^*_2ScCH_2CH_2C_6H_5$ and various concentrations of 2-butyne. Plotting the observed rate constants, $k_{obs}$, obtained from these experiments vs the concentration of added 2-butyne gave a line with slope $1.4 \times 10^{-6}$ with deviations from the line of less than 10%. After the reaction rate was determined to be independent of 2-butyne concentration over the range 0.6-3.0 M, all subsequent kinetic runs were carried out with a butyne concentration in this range. Rate constants were obtained for each complex at several different temperatures. Activation parameters were derived from an Eyring plot as described previously.

**Deuterium Kinetic Isotope Effect of β-Hydrogen Elimination.** $Cp^*_2ScCH_2CHDC_6H_5$ (ca. 25 mg) was loaded into a sealable NMR tube with 0.5 mL of toluene-$d_8$. A calibrated gas volume was attached to the tube. The solution was degassed at -78 °C; butyne (ca. 10 equiv) was condensed at -196 °C. The tube was allowed to stand at room temperature for 5 h. The $^1H$ NMR spectrum (400 MHz) was recorded; the terminal vinyl resonances for styrene-$d_0$ and styrene-$d_1$ were cut from the spectrum and weighed. The isotope effect ($k_H/k_D$) was calculated from the ratio of areas of the cut and weighed peaks.

**Acknowledgment.** This work was supported by the USDOE Office of Basic Energy Research, Office of Basic Energy Sciences (Grant No. DE-FG03-85ER13431) and by the Shell Companies Foundation, which are gratefully acknowledged. The use of the Southern California Regional NMR Facility, supported by the National Science Foundation Grant No. CHE-84-40137 is also gratefully acknowledged. W.D.C. also thanks the National Science Foundation for an NSF Predoctoral Fellowship (1987-1990). We thank Dr. Jay A. Labinger for helpful discussions.

# Oxygenation and Oxidative Coupling Processes of Alkyl Ligands of *cis*-Dialkylcobalt(III) Complexes with Dioxygen Catalyzed by Coenzyme Analogues in the Presence of Perchloric Acid

**Kunio Ishikawa,[1a] Shunichi Fukuzumi,*[1b] Tatsushi Goto, and Toshio Tanaka[1c]**

*Contribution from the Department of Applied Chemistry, Faculty of Engineering, Osaka University, Suita, Osaka 565, Japan.* *Received June 27, 1989*

**Abstract:** Oxygenation of the benzyl ligand of *cis*-$[(PhCH_2)_2Co(bpy)_2]^+$ (bpy = 2,2'-bipyridine) occurs efficiently in the presence of a catalytic amount of a coenzyme analogue, riboflavin, riboflavin-2',3',4',5'-tetraacetate, lumazine, or aminopterin, in acetonitrile containing perchloric acid at 298 K to produce benzyl hydroperoxide, which decomposes to yield benzaldehyde as the final oxygenated product. In the case of *cis*-$[R_2Co(bpy)_2]^+$ (R = Et, Me), however, no oxygenation of the ligands proceeds under the same conditions; instead, oxidative coupling of the alkyl ligands of *cis*-$[R_2Co(bpy)_2]^+$ takes place in the coenzyme-catalyzed oxidation by dioxygen to yield ethane and butane, respectively, when dioxygen is reduced to hydrogen peroxide. The origin of such a difference in the oxygenation and oxidative coupling pathways depending on the alkyl ligands is discussed based on the comparison of the products and kinetics with those of the one-electron oxidation of *cis*-$[R_2Co(bpy)_2]^+$ by various oxidants in the absence and presence of dioxygen in acetonitrile at 298 K.

The interaction of dioxygen with transition-metal complexes has been extensively studied owing to the importance in understanding the mode of action of biological oxygen carriers.[2] In contrast, the contact of dioxygen with air-sensitive organometallic compounds has usually been avoided deliberately on their handling. Thus, relatively little is known about the reactions of dioxygen with such organometallic compounds, although dioxygenation reactions of alkyl Grignard reagents have been known for a long time,[3] and the chemistry of organometallic compounds containing oxo and peroxo ligands formed in the reactions with dioxygen has recently attracted increasing interest with relevance to selective catalytic oxidation processes.[4-8] Moreover, reactions of most

(1) (a) Current address: Dental School, Tokushima University, Tokushima 770, Japan. (b) To whom correspondence should be addressed at Osaka University. (c) Current address: Department of Applied Physics and Chemistry, Fukui Institute of Technology, Fukui 910, Japan.

(2) (a) Vaska, L. *Acc. Chem. Res.* **1976**, *9*, 175. (b) Collman, J. P. *Ibid.* **1977**, *10*, 265. (c) McLendon, G.; Martell, A. E. *Coord. Chem. Rev.* **1976**, *19*, 1. (d) Jones, R. D.; Summerville, D. A.; Basolo, F. *Chem. Rev.* **1979**, *79*, 139.

(3) (a) Porter, C. W.; Steele, C. *J. Am. Chem. Soc.* **1920**, *42*, 2650. (b) Walling, C.; Buckler, S. A. *J. Am. Chem. Soc.* **1953**, *75*, 4372. (c) Walling, C.; Buckler, S. A. *Ibid.* **1955**, *77*, 6032.

0002-7863/90/1512-1577$02.50/0 

air-sensitive organometallic compounds with dioxygen are too rapid to study the mechanisms in detail.[9] However, some organometallic compounds such as alkylcobalt(III) complexes are rather stable to dioxygen. In such a case, oxygenation reactions of stable organometallic compounds require irradiation of light.[10-12] The oxygenation of alkyl ligands of monoalkylcobalt(III) complexes (RCo) are known to be induced also by thermal homolytic cleavage of cobalt–carbon bonds (eq 1),[13] followed by the reactions of the dissociated alkyl radicals with dioxygen (eq 2).[14] In other cases,

$$\mathrm{RCo} \rightleftarrows (\mathrm{R^{\bullet}\ Co}) \qquad (1)$$

$$(\mathrm{R^{\bullet}\ Co}) + \mathrm{O_2} \rightarrow \mathrm{ROO^{\bullet}} + \mathrm{Co} \qquad (2)$$

oxidation of dialkylmetal complexes ($R_2M$) by dioxygen leads to oxidative coupling of the alkyl ligands (eq 3).[15,16] In any case,

$$\mathrm{R_2M} + \mathrm{O_2} \rightarrow \mathrm{R\text{-}R} + \mathrm{M^+} + \mathrm{O_2^-} \qquad (3)$$

however, there have so far been no reports on catalytic systems to accelerate the reactions of organometallic compounds with dioxygen. In biological systems, redox coenzymes such as flavins and pterins are well-known to play important roles in the enzymatic oxidation of substrates by dioxygen.[17,18]

In this study,[19] we report efficient catalytic systems for the reactions of *cis*-$[R_2Co(bpy)_2]^+$ (R = $PhCH_2$, Et, Me; bpy = 2,2′-bipyridine)[20] with dioxygen using redox coenzyme analogues, riboflavin, riboflavin-2′,3′,4′,5′-tetraacetate, lumazine (pteridine-2,4-diol), and aminopterin (4-aminofolic acid), as catalysts in the presence of $HClO_4$ in acetonitrile (MeCN). In the coenzyme-catalyzed oxidation of *cis*-$[R_2Co(bpy)_2]^+$ by dioxygen, both oxygenation and oxidative coupling processes occur depending on the difference in the alkyl ligands. The products as well as the kinetics are compared with those of electron-transfer reactions from *cis*-$[R_2Co(bpy)_2]^+$ to various one-electron oxidants in order to elucidate the origin of the different oxidation pathways by dioxygen–oxygenation and oxidative coupling processes, depending on the alkyl ligands of *cis*-$[R_2Co(bpy)_2]^+$.

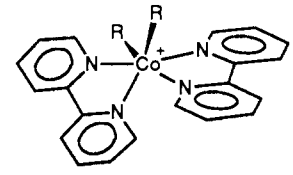

*cis*-$[R_2Co(bpy)_2]^+$ (ref 20)

## Experimental Section

**Materials.** *cis*-Dialkylcobalt(III) complexes, *cis*-$[R_2Co(bpy)_2]ClO_4$ (R = $PhCH_2$, Et, Me), were prepared by the reaction of $CoCl_2 \cdot 6H_2O$ with an excess of $NaBH_4$ in the presence of the corresponding alkyl halide and the ligand bpy.[21,22] They were isolated as the perchlorate salts and recrystallized from methanol–water. The purity of the complexes was checked by elemental analysis and $^1H$ NMR (100 MHz). Anal. Calcd for $C_{34}H_{30}N_4O_4CoCl$ (*cis*-$[(PhCH_2)_2Co(bpy)_2]ClO_4$): C, 63.0; H, 4.7; N, 8.7. Found: C, 62.0; H, 4.6; N, 8.5. $^1H$ NMR ($CD_3CN$) $\delta$ 3.54 (q, 4 H), 6.33–6.86 (m, 10 H), 7.02–8.53 (m, 16 H). Anal. Calcd for $C_{24}H_{28}N_4O_4CoCl$ (*cis*-$[Et_2Co(bpy)_2]ClO_4$): C, 52.7; H, 5.2; N, 10.2. Found: C, 52.1; H, 5.1; N, 10.0. $^1H$ NMR ($CD_3CN$) $\delta$ 0 (t, 6 H), 1.62 (m, 4 H), 7.09–8.69 (m, 16 H). Anal. Calcd for $C_{22}H_{22}N_4O_4CoCl$ (*cis*-$[Me_2Co(bpy)_2]ClO_4$): C, 52.8; H, 4.4; N, 11.2. Found: C, 52.7; H, 4.6; N, 11.1. $^1H$ NMR ($CD_3CN$) $\delta$ 0.71 (s, 6 H), 7.26–8.76 (m, 16 H). Riboflavin-2′,3′,4′,5′-tetraacetate was prepared by the reaction of riboflavin with acetic anhydride in pyridine and purified by recrystallization from an ethanol–chloroform mixture.[23] Riboflavin, lumazine, and aminopterin were obtained commercially and purified by the standard procedure. Perchloric acid (70% aqueous solution) was purchased from Wako Pure Chemicals and stored under nitrogen. Tetracyanoethylene (TCNE), 2,3-dichloro-5,6-dicyano-*p*-benzoquinone (DDBQ), and 7,7,8,8-tetracyano-*p*-quinodimethane (TCNQ) were also obtained commercially and purified by the standard method.[24] 2,3-Dicyano-*p*-benzoquinone (DCBQ) was prepared from the corresponding hydroquinone according to the literature.[25] The syntheses of $[Fe(phen)_3](ClO_4)_3$ (phen = 1,10-phenanthroline) and $[Fe(bpy)_3](ClO_4)_3$ were described elsewhere.[26] Ferrocenium, *n*-butylferrocenium, and 1,1′-dimethylferrocenium ions were prepared by the oxidation of the corresponding ferrocene derivatives with *p*-benzoquinone in the presence of perchloric acid in acetonitrile[27] and isolated as the hexafluorophosphate salts. Benzyl hydroperoxide used as the authentic sample was prepared by the addition of benzylmagnesium chloride to dioxygen-saturated ether at −70 °C.[3] $[Co(bpy)_3](ClO_4)_3$ was prepared by the reaction of $Co(ClO_4)_3 \cdot 6H_2O$ with an excess amount of 2,2′-bipyridine ligand. Reagent grade acetonitrile was purified by the standard procedure,[24] followed by redistillation from calcium hydride. Acetonitrile-$d_3$ was stirred with freshly activated molecular sieves 4A (Wako Pure Chemicals) and then transferred under vacuum into a dry, glass-stoppered bottle. Other reagents used for the product analysis were obtained commercially.

**Product Analysis.** Typically, a catalytic amount of riboflavin-2′,3′,4′,5′-tetraacetate ($1.0 \times 10^{-6}$ mol) was added to an NMR tube that contained an oxygen-saturated acetonitrile-$d_3$ (0.6 $cm^3$) solution of

(4) (a) Parkin, G.; Bercaw, J. E. *J. Am. Chem. Soc.* **1989**, *111*, 393. (b) van Asselt, A.; Trimmer, M. S.; Henling, L. M.; Bercaw, J. E. *Ibid.* **1988**, *110*, 8254.

(5) (a) Bottomley, F.; Magill, C. P.; White, P. S. *J. Am. Chem. Soc.* **1989**, *111*, 3070. (b) Bottomley, F.; Paez, D. E.; White, P. S. *Ibid.* **1985**, *107*, 7226. (c) Bottomley, F.; Darkwa, J.; Sutin, L.; White, P. S. *Organometallics* **1986**, *5*, 2165. (d) Bottomley, F.; Drummond, D. F.; Paez, D. E.; White, P. S. *J. Chem. Soc., Chem. Commun.* **1986**, 1752. (e) Bottomley, F.; Sutin, L. *Ibid.* **1987**, 1112.

(6) (a) Morse, D. B.; Rauchfuss, T. B.; Wilson, S. R. *J. Am. Chem. Soc.* **1988**, *110*, 8234. (b) Faller, J. W.; Ma, Y. *Organometallics* **1988**, *7*, 559; Legzdins, P.; Phillips, E. C.; Rettig, S. J.; Sanchez, L.; Trotter, J.; Yee, V. C. *Ibid.* **1988**, *7*, 1877.

(7) (a) Herrmann, W. A. *J. Organomet. Chem.* **1986**, *300*, 111. (b) Holm, R. H. *Chem. Rev.* **1987**, *87*, 1401. (c) Mimoun, H. *The Chemistry of Functional Groups, Peroxides*; Patai, S., Ed.; Wiley: New York, 1983; p 465.

(8) Sheldon, R. A.; Kochi, J. K. *Metal-Catalyzed Oxidation of Organic Compounds*; Academic Press: New York, 1981.

(9) Kochi, J. K. *Organometallic Mechanisms and Catalysis*; Academic Press: New York, 1978.

(10) (a) Carlton, L.; Lindsell, W. E.; Preston, P. N. *J. Chem. Soc., Dalton Trans.* **1982**, 1483. (b) Fukuzumi, S.; Kuroda, S.; Tanaka, T. *J. Chem. Soc., Perkin Trans. 2* **1986**, 25.

(11) Kendrick, M. J.; Al-Akhdar, W. *Inorg. Chem.* **1987**, *26*, 3972.

(12) (a) Schrauzer, G. N.; Lee, L. P.; Sibert, J. W. *J. Am. Chem. Soc.* **1970**, *92*, 2997. (b) Nishinaga, A.; Nishizawa, K.; Nakayama, Y.; Matsuura, T. *Tetrahedron Lett.* **1977**, 85. (c) Bied-Charreton, C.; Gaudemer, A. *J. Organomet. Chem.* **1977**, *124*, 299. (d) Merienne, C.; Giannotti, C.; Gaudemer, A. *Ibid.* **1973**, *54*, 281.

(13) (a) Halpern, J. *Acc. Chem. Res.* **1982**, *15*, 238. (b) Halpern, J. *Bull. Chem. Soc. Jpn.* **1988**, *61*, 13.

(14) (a) Blau, R. J.; Espenson, J. H. *J. Am. Chem. Soc.* **1985**, *107*, 3530. (b) Schrauzer, G. N.; Grate, J. H. *Ibid.* **1981**, *103*, 541.

(15) (a) Whitesides, G. M.; Filippo, J. S., Jr.; Casey, C. P.; Panek, E. J. *J. Am. Chem. Soc.* **1967**, *89*, 5302. (b) Whitesides, G. M.; Fischer, W. F., Jr.; Filippo, J. S., Jr.; Bashe, R. W.; House, H. O. *Ibid.* **1969**, *91*, 4871.

(16) (a) Komiya, S.; Albright, T. A.; Hoffmann, R.; Kochi, J. K. *J. Am. Chem. Soc.* **1977**, *99*, 8440. (b) Morrell, D. G.; Kochi, J. K. *Ibid.* **1975**, *97*, 7262. (c) Wada, M.; Kusabe, K.; Oguro, K. *Inorg. Chem.* **1977**, *16*, 446.

(17) (a) Bruice, T. C. *Acc. Chem. Res.* **1980**, *13*, 256. (b) Walsh, C. *Ibid.* **1980**, *13*, 148.

(18) Fukuzumi, S.; Tanaka, T. *Photoinduced Electron Transfer*; Fox, M. A., Chanon, M., Eds.; Elsevier: Amsterdam, 1988; Part C, Chapter 11.

(19) A preliminary report has appeared: Fukuzumi, S.; Goto, T.; Ishikawa, K.; Tanaka, T. *Chem. Lett.* **1988**, 1923.

(20) The structural drawing of *cis*-$[R_2Co(bpy)_2]ClO_4$ is made assuming that the stereochemistry of the ligands around the cobalt is the same as that in the reported structure of *cis*-$[R_2Fe(bpy)_2]$. See: Lau, W.; Huffman, J. C.; Kochi, J. K. *Organometallics* **1982**, *1*, 155. The cis configuration of the complexes has been supported by a nonequivalence of the hydrogen atoms in the 6- and 6′-positions of the bipyridine groups in the $^1H$ NMR spectra; see ref 22.

(21) (a) Fukuzumi, S.; Ishikawa, K.; Tanaka, T. *J. Chem. Soc., Dalton Trans.* **1985**, 899. (b) Fukuzumi, S.; Ishikawa, K.; Tanaka, T. *Nippon Kagaku Kaishi* **1985**, 62.

(22) Mestroni, G.; Camus, A.; Mestroni, E. *J. Organomet. Chem.* **1970**, *24*, 775.

(23) Kyogoku, Y.; Yu, B. S. *Bull. Chem. Soc. Jpn.* **1969**, *42*, 1387.

(24) Perrin, D. D.; Armarego, W. L. F.; Perrin, D. R. *Purification of Laboratory Chemicals*; Pergamon Press: New York, 1966.

(25) (a) Cason, J.; Allen, C. F.; Goodwin, S. *J. Org. Chem.* **1948**, *13*, 403. (b) Brook, A. G. *J. Chem. Soc.* **1953**, 5040.

(26) (a) Fukuzumi, S.; Nishizawa, N.; Tanaka, T. *Bull. Chem. Soc. Jpn.* **1982**, *55*, 3482. (b) Ford-Smith, M. H.; Sutin, N. *J. Am. Chem. Soc.* **1961**, *83*, 1830.

(27) Fukuzumi, S.; Ishikawa, K.; Hironaka, K.; Tanaka, T. *J. Chem. Soc., Perkin Trans. 2* **1987**, 751.

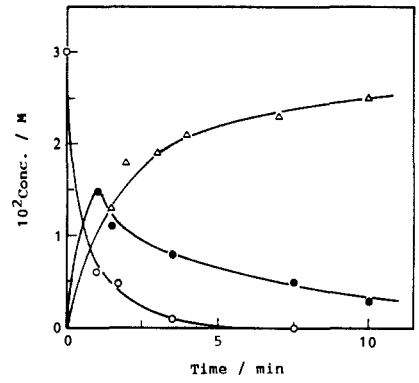


**Figure 1.** Oxygenation of the benzyl ligand of *cis*-[$(PhCH_2)_2Co(bpy)_2$]$^+$ ($3.0 \times 10^{-2}$ M) in the presence of $HClO_4$ ($1.2 \times 10^{-1}$ M) and a catalytic amount of lumazine ($5.3 \times 10^{-3}$ M) in $CD_3CN$ at 298 K: *cis*-[$(PhCH_2)_2Co(bpy)_2$]$^+$ (○); $PhCH_2OOH$ (●); PhCHO (△).

*cis*-[$R_2Co(bpy)_2$]$ClO_4$ ($1.8 \times 10^{-5}$ mol). The reaction was started by adding $HClO_4$ ($6.0 \times 10^{-5}$ mol) with a micropipet under a stream of dioxygen. Then the NMR tube was sealed by a rubber septum and the reaction was monitored by using a Japan Electron Optics JNM-PS-100 $^1H$ NMR spectrometer (100 MHz). The amounts of $PhCH_2OOH$ and [$PhCH_2Co(bpy)_2$]$^{2+}$ formed were determined by the appearance of new signals at $\delta$ (ppm) 4.89 (2 H, s) and 2.90 (2 H, s) due to the methylene protons of the benzyl groups, respectively. After completion of the reaction, the products were analyzed also by GLC using a Unibeads 1-S or a Gaskropak 54 column.

**Kinetic Measurements.** Kinetic measurements were carried out by using a Union RA-103 stopped-flow spectrophotometer and a Union SM-401 spectrophotometer for the oxidation of *cis*-[$R_2Co(bpy)_2$]$^+$ with half-lives of shorter than 10 s and much longer than 10 s, respectively. Rates of the coenzyme-catalyzed oxidation of *cis*-[$R_2Co(bpy)_2$]$^+$ by dioxygen and electron transfer from *cis*-[$R_2Co(bpy)_2$]$^+$ to ferrocenium ions were monitored by the rate of disappearance of absorbance at $\lambda_{max}$ due to *cis*-[$R_2Co(bpy)_2$]$ClO_4$ in MeCN ($\lambda_{max}$ = 502, 495, and 472 nm for R = $PhCH_2$, Et, and Me, respectively). Rates of electron transfer from *cis*-[$R_2Co(bpy)_2$]$^+$ to organic one-electron oxidants were monitored by the increase in absorbance at $\lambda_{max}$ due to the radical anions [$\lambda_{max}$ 457 nm, $\epsilon_{max}$ $5.67 \times 10^3$ $M^{-1}$ $cm^{-1}$ for the radical anion of tetracyanoethylene (TCNE),[28] $\lambda_{max}$ 585 nm, $\epsilon_{max}$ $5.46 \times 10^3$ $M^{-1}$ $cm^{-1}$ for the radical anion of 2,3-dichloro-5,6-dicyano-*p*-benzoquinone (DDBQ),[29] $\lambda_{max}$ 585 nm, $\epsilon_{max}$ $3.63 \times 10^3$ $M^{-1}$ $cm^{-1}$ for the radical anion of 2,3-dicyano-*p*-benzoquinone (DCBQ),[29] and $\lambda_{max}$ 842 nm, $\epsilon_{max}$ $4.33 \times 10^4$ $M^{-1}$ $cm^{-1}$ for the radical anion of 7,7,8,8-tetracyano-*p*-quinodimethane (TCNQ)[30]]. All kinetic measurements were carried out under pseudo-first-order conditions where the concentrations of oxidants and $HClO_4$ were maintained at >10-fold excess of the concentration of *cis*-[$R_2Co(bpy)_2$]$^+$ at 298 K. Pseudo-first-order rate constants were determined by least-squares curve fits using a Union System 77 or NEC 9801 $VM_2$ microcomputer.

**Electron Spin Resonance Measurements.** Typically, a small amount of *cis*-[$R_2Co(bpy)_2$]$^+$ ($2.0 \times 10^{-7}$ mol) was added to a quartz ESR tube (1-mm i.d.) equipped with a side arm that contained an MeCN solution (0.20 $cm^3$) of Fl ($1.0 \times 10^{-3}$ M) and $HClO_4$ ($1.0 \times 10^{-2}$ M). After the ESR tube with the side arm was sealed and the reactant solution in the side arm was thoroughly degassed under vacuum by successive freeze–pump–thaw cycles, the solution was transferred to the ESR tube. Then the ESR spectra were recorded under a nonsaturating microwave power condition with a modulation amplitude $8.0 \times 10^{-2}$ mT using a JEOL X-band spectrometer (JES-ME-LX) at room temperature. The further reduction of modulation amplitude did not improve the hyperfine resolution. The *g* value and the hyperfine coupling constants (hfc) of the ESR spectra were calibrated by using an $Mn^{2+}$ marker. The simulation of the ESR spectra was performed with a NEC 9801 $VM_2$ microcomputer.

## Results

**Coenzyme-Catalyzed Oxygenation of the Benzyl Ligand of *cis*-[$(PhCH_2)_2Co(bpy)_2$]$^+$.** *cis*-[$(PhCH_2)_2Co(bpy)_2$]$ClO_4$ shows no reactivity toward dioxygen or redox coenzyme analogues, riboflavin (Fl), riboflavin-2′,3′,4′,5′-tetraacetate (FlTA), lumazine (L), and aminopterin (AP), in MeCN at 298 K. When a strong acid such as perchloric acid ($HClO_4$) is added to an oxygen-saturated MeCN solution of *cis*-[$(PhCH_2)_2Co(bpy)_2$]$^+$ in the presence of a catalytic amount of coenzyme analogue, however, *cis*-[$(PhCH_2)_2Co(bpy)_2$]$^+$ is readily oxidized by dioxygen to produce benzyl hydroperoxide (eq 4). A typical example of the

$$cis\text{-}[(PhCH_2)_2Co(bpy)_2]^+ + O_2 + H^+ \xrightarrow{\text{Fl, FlTA, L, or AP}} [PhCH_2Co(bpy)_2]^{2+} + PhCH_2OOH \quad (4)$$

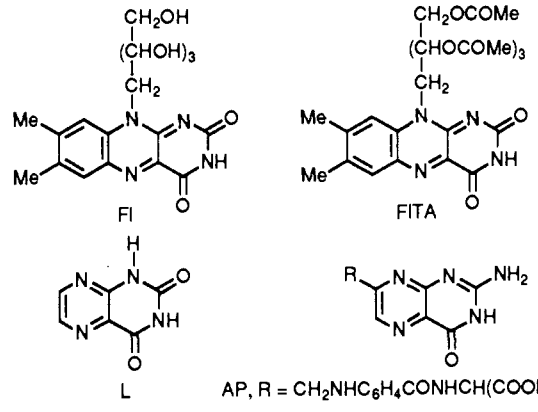


coenzyme-catalyzed oxygenation reaction of *cis*-[$(PhCH_2)_2Co(bpy)_2$]$^+$ is shown in Figure 1, where *cis*-[$(PhCH_2)_2Co(bpy)_2$]$^+$ ($3.0 \times 10^{-2}$ M) reacts with dioxygen ($6.9 \times 10^{-5}$ mol) in the presence of a catalytic amount of lumazine ($5.3 \times 10^{-3}$ M) in $CD_3CN$ (0.60 $cm^3$) containing $HClO_4$ (0.12 M) to produce $PhCH_2OOH$, which decomposes to yield benzaldehyde (PhCHO) as the final oxygenated product.[31] The formation of [$PhCH_2Co(bpy)_2$]$^{2+}$ (eq 4) is also confirmed by the $^1H$ NMR spectrum (see Experimental Section). Other redox coenzyme analogues (FlTA, Fl, and AP) can also catalyze the oxygenation of the benzyl ligand of *cis*-[$(PhCH_2)_2Co(bpy)_2$]$^+$ in the presence of $HClO_4$ in MeCN at 298 K, and the yields of benzaldehyde are summarized in Table I.

**Table I.** Product Yields in the Coenzyme-Catalyzed Oxidation of *cis*-[$(PhCH_2)_2Co(bpy)_2$]$^+$ [$(1.8–2.5) \times 10^{-5}$ mol] by Dioxygen in the Presence and Absence of $HClO_4$ in $CD_3CN$ (0.60 $cm^3$) at 298 K

| amt, $10^{-5}$ mol | | | |
|---|---|---|---|
| $O_2$ | catalyst[a] | $HClO_4$ | products (yield,[b] %) |
| | FlTA | | |
| 6.9 | 0 | 0 | no reaction |
| 0 | 0.10 | 0 | no reaction |
| 6.9 | 0.10 | 0 | no reaction |
| 6.9 | 0.10 | 6.0 | PhCHO (99), $PhCH_2OOH$ (trace) |
| 0 | 0 | 6.0 | $PhCH_3$ (100) |
| | Fl | | |
| 6.9 | 0.10 | 6.0 | PhCHO (100), $PhCH_2OOH$ (trace) |
| 0 | 3.0 | 6.0 | $PhC_2H_4Ph$ (50) |
| | L | | |
| 6.9 | 0.32 | 7.2 | PhCHO (100), $PhCH_2OOH$ (trace) |
| | AP | | |
| 6.9 | 0.32 | 6.0 | PhCHO (100), $PhCH_2OOH$ (trace) |

[a] Catalyst: riboflavin-2′,3′,4′,5′-tetraacetate (FlTA), riboflavin (Fl), lumazine (L), aminopterin (AP). [b] Based on the amount of *cis*-[$(PhCH_2)_2Co(bpy)_2$]$^+$.

Flavin analogues are known to be protonated at the N-1 position in a strongly acidic aqueous solution ($pK_a$ = 0).[32] In MeCN,

(28) (a) Webster, O. W.; Mahler, W.; Benson, R. E. *J. Am. Chem. Soc.* **1962**, *84*, 3678. (b) Fukuzumi, S.; Kondo, Y.; Tanaka, T. *J. Chem. Soc., Perkin Trans. 2* **1984**, 673.

(29) (a) Iida, Y. *Bull. Chem. Soc. Jpn.* **1971**, *44*, 1777. (b) Fukuzumi, S.; Nishizawa, N.; Tanaka, T. *J. Org. Chem.* **1984**, *49*, 3571.

(30) Melby, L. R.; Harder, R. J.; Hertler, W. R.; Mahler, W.; Benson, R. E.; Mochel, W. E. *J. Am. Chem. Soc.* **1962**, *84*, 3374.

(31) The decomposition of $PhCH_2OOH$ to PhCHO occurs in the presence of $HClO_4$ in MeCN. See: Fukuzumi, S.; Ishikawa, K.; Tanaka, T. *Chem. Lett.* **1986**, 1.

(32) Hemmerich, P.; Veeger, C.; Wood, H. C. S. *Angew. Chem.* **1965**, *77*, 699. Dudley, K. H.; Ehrenberg, A.; Hemmerich, P.; Müller, F. *Helv. Chim. Acta* **1964**, *47*, 1354.

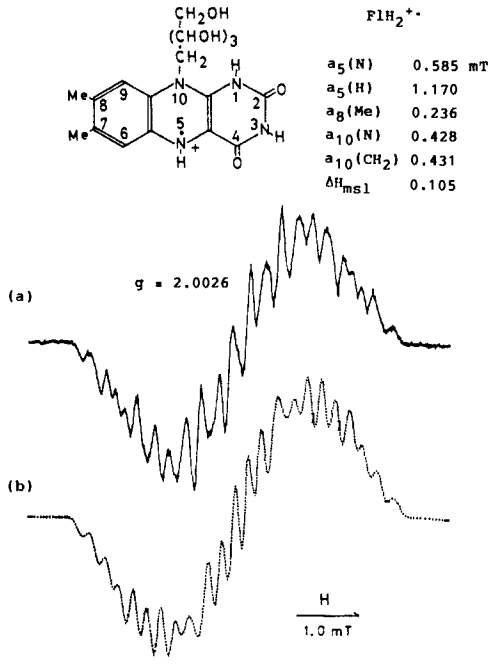


**Figure 2.** (a) ESR spectrum of $FlH_2^{\cdot+}$ formed in the oxidation of *cis*-$[(PhCH_2)_2Co(bpy)_2]^+$ ($1.0 \times 10^{-3}$ M) with $FlH^+$ ($1.0 \times 10^{-3}$ M) in the presence of $HClO_4$ ($1.0 \times 10^{-2}$ M) in deaerated MeCN at 298 K and (b) the computer simulation spectrum of $FlH_2^{\cdot+}$.

the protonation of flavin analogues occurs much more readily than that in $H_2O$.[19,33] The protonation equilibrium constant $K$ of Fl in MeCN has been reported to be $2.7 \times 10^6$ $M^{-1}$.[33] Thus, the absorption band due to Fl and FlTA (ca. $10^{-4}$ M) in MeCN ($\lambda_{max}$ 439 and 442 nm) is blue shifted in the presence of even slightly excess $HClO_4$ ($\lambda_{max}$ 388 and 390 nm, respectively). Such a blue shift due to the protonation is observed also for lumazine or aminopterin. Thus, all coenzyme analogues (Fl, FlTA, L, and AP) exist in the protonated form ($FlH^+$, $FlTAH^+$, $LH^+$, and $APH^+$) in the presence of an excess amount of $HClO_4$ in MeCN as shown in the case of Fl (eq 5).

$$Fl + H^+ \overset{K}{\rightleftharpoons} FlH^+ \quad (5)$$

In the absence of dioxygen, the stoichiometric oxidation of *cis*-$[R_2Co(bpy)_2]^+$ ($R = PhCH_2$) by $FlH^+$ occurs in the presence of $HClO_4$ in MeCN to yield the coupling product, $PhC_2H_4Ph$ (Table I). The stoichiometry of the reaction is given by eq 6, where

$$cis\text{-}[R_2Co(bpy)_2]^+ + 2FlH^+ + 2H^+ \rightarrow R\text{-}R + [Co(bpy)_2]^{3+} + 2FlH_2^{\cdot+} \quad (6)$$

formation of $FlH_2^{\cdot+}$ is confirmed by the appearance of the ESR spectrum as shown in Figure 2 (part a). A computer simulation spectrum of $FlH_2^{\cdot+}$ is also shown in Figure 2 (part b) with the hyperfine coupling constant (hfc) best-fit parameters $a_5(N)$ = 0.585, $a_5(H)$ = 1.170, $a_8(Me)$ = 0.236, $a_{10}(N)$ = 0.428, and $a_{10}(CH_2)$ = 0.431 mT and the maximum slope line width $\Delta H_{msl}$ = 0.105 mT. The simulated spectrum agrees well with the observed spectrum, except for some line intensities. The large hfc value due to the N-5 proton and the lack of appreciable hfc due to C-6 and C-9 protons are characteristic of a dihydroflavin radical cation.[34] The lack of appreciable hfc due to the C-7 proton, N-1, or N-3 is typical for flavin radical species [flavosemiquinone radical anion ($Fl^{\cdot-}$), neutral flavosemiquinone ($FlH^{\cdot}$), and dihydroflavin radical cation ($FlH_2^{\cdot+}$)][34] as confirmed by the MO calculation.[35] A similar ESR spectrum due to $FlTAH_2^{\cdot+}$ is obtained in the oxidation of *cis*-$[R_2Co(bpy)_2]^+$ by $FlTAH^+$ in the presence of $HClO_4$ in deaerated MeCN.[36] Both $FlH_2^{\cdot+}$ ($\lambda_{max}$ 500 nm) and

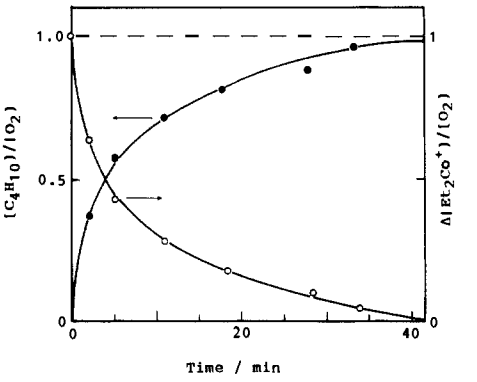


**Figure 3.** Plots of the ratios of the amount of $C_4H_{10}$ formed in the $FlH^+$-catalyzed oxidation of *cis*-$[Et_2Co(bpy)_2]^+$ ($3.59 \times 10^{-5}$ mol) with dioxygen ($1.38 \times 10^{-5}$ mol) in the presence of $HClO_4$ ($6.8 \times 10^{-5}$ mol) and $H_2O$ ($5.4 \times 10^{-4}$ mol) in $CD_3CN$ (0.60 $cm^3$) and that of *cis*-$[Et_2Co(bpy)_2]^+$ reacted to the initial amount of $O_2$ vs reaction time.

$FlTAH_2^{\cdot+}$ ($\lambda_{max}$ 504 nm) are very stable in the presence of $HClO_4$ even in oxygen-saturated MeCN.

In the reaction of $LH^+$ with *cis*-$[(PhCH_2)_2Co(bpy)_2]^+$ as well, a transient new absorption band due to $LH_2^{\cdot+}$ ($\lambda_{max}$ 416 nm)[37] is observed. In the case of $APH^+$, however, no free radical species derived from $APH^+$ has been detected in the reaction with *cis*-$[(PhCH_2)_2Co(bpy)_2]^+$ in the presence of $HClO_4$ in deaerated MeCN.

In the absence of dioxygen and coenzyme analogues, the cobalt–carbon bond of *cis*-$[(PhCH_2)_2Co(bpy)_2]^+$ is cleaved by the electrophilic attack of proton to yield $[PhCH_2Co(bpy)_2]^{2+}$ and toluene (eq 7) (Table I).

$$cis\text{-}[(PhCH_2)_2Co(bpy)_2]^+ + H^+ \rightarrow PhCH_3 + [PhCH_2Co(bpy)_2]^{2+} \quad (7)$$

**Coenzyme-Catalyzed Oxidative Coupling of Alkyl Ligands of *cis*-$[R_2Co(bpy)_2]^+$ (R = Et, Me) by Dioxygen.** The coenzyme-catalyzed oxidation of other *cis*-dialkylcobalt(III) complexes, *cis*-$[R_2Co(bpy)_2]^+$ (R = Me, Et), by dioxygen also proceeds efficiently in the presence of $HClO_4$ in MeCN. In this case, however, no oxygenation of the alkyl ligands occurs, but instead coupling products of the alkyl groups are obtained upon the catalytic oxidation of *cis*-$[R_2Co(bpy)_2]^+$ by dioxygen in the presence of $HClO_4$. A typical example is shown in Figure 3, where the ratios of the amount of the coupling product $C_4H_{10}$ formed in the $FlTAH^+$-catalyzed oxidation of *cis*-$[Et_2Co(bpy)_2]^+$ by dioxygen and the amount of *cis*-$[Et_2Co(bpy)_2]^+$ reacted to the initial amount of dioxygen are plotted against the reaction time. The reaction is carried out in the presence of a catalytic amount of FlTA ($2.9 \times 10^{-6}$ mol) in $CD_3CN$ containing $HClO_4$ ($6.8 \times 10^{-5}$ mol) and $H_2O$ ($5.40 \times 10^{-4}$ mol) under the condition that the initial amount of *cis*-$[Et_2Co(bpy)_2]^+$ ($3.59 \times 10^{-5}$ mol) is in excess to that of dioxygen ($1.38 \times 10^{-5}$ mol).[38] Figure 3 indicates that the stoichiometry of the catalytic oxidation of *cis*-$[Et_2Co(bpy)_2]^+$ by dioxygen in the presence of $HClO_4$ is given by eq 8.[39]

$$cis\text{-}[(C_2H_5)_2Co(bpy)_2]^+ + O_2 + 2H^+ \xrightarrow{FlTA} C_4H_{10} + [Co(bpy)_2]^{3+} + H_2O_2 \quad (8)$$

The yields of the coupling products in other coenzyme-catalyzed oxidations of *cis*-$[R_2Co(bpy)_2]^+$ (R = Et, Me; $(2.1\text{–}3.6) \times 10^{-5}$ mol) by an excess amount of dioxygen ($6.9 \times 10^{-5}$ mol) are shown in Table II. In the case of R = Me, the coupling product, ethane,

(33) Fukuzumi, S.; Kuroda, S.; Goto, T.; Ishikawa, K.; Tanaka, T. *J. Chem. Soc., Perkin Trans. 2* **1989**, 1047.
(34) Müller, F.; Hemmerich, P.; Ehrenberg, A. *Flavins and* Flavoproteins; Kamin, H., Ed.; University Park Press: Baltimore, 1971; p 107.
(35) Guzzo, A. V.; Tollin, G. *Arch. Biochem. Biophys.* **1963**, *103*, 231.
(36) The best-fit ESR parameters are $a_5(N)$ = 0.630, $a_5(H)$ = 1.411, $a_8(Me)$ = 0.305, $a_{10}(N)$ = 0.477, and $a_{10}(CH_2)$ = 0.477 mT and the maximum slope line width $\Delta H_{msl}$ = 0.080 mT.
(37) Fukuzumi, S.; Tanii, K.; Tanaka, T. *Chem. Lett.* **1989**, 35.
(38) The $H_2O$ is added to the reaction system in order to slow down the reaction rate. Such a retarding effect of $H_2O$ on acid-catalyzed redox reactions in MeCN has recently been reported. See: Fukuzumi, S.; Chiba, M.; Tanaka, T. *Chem. Lett.* **1989**, 31.
(39) The $[Co(bpy)_2]^{3+}$ formed is converted to $[Co(bpy)_3]^{3+}$, which is the most stable form of the cobalt(III) complexes with bpy ligands. See: Fukuzumi, S.; Ishikawa, K.; Tanaka, T. *Organometallics* **1987**, *6*, 358.

**Table II.** Product Yields in the Coenzyme-Catalyzed Oxidation of *cis*-[$R_2Co(bpy)_2$]$^+$ (R = Et, Me) by Dioxygen in the Presence and Absence of $HClO_4$ in $CD_3CN$ (0.60 $cm^3$) at 298 K

| amt, $10^{-5}$ mol | | | | |
|---|---|---|---|---|
| *cis*-[$R_2Co(bpy)_2$]$^+$ | $O_2$ | catalyst | $HClO_4$ | products (yield,[a] %) |
| | | FlTA | | |
| R = Et | | | | |
| 2.1 | 6.9 | 0 | 0 | no reaction |
| 2.1 | 0 | 0.28 | 0 | no reaction |
| 2.4 | 6.9 | 0.28 | 6.8 | $C_4H_{10}$ (100), $C_2H_6$ (trace) |
| | | Fl | | |
| 2.4 | 6.9 | 0.28 | 6.8 | $C_4H_{10}$ (100), $C_2H_6$ (trace) |
| | | L | | |
| 2.4 | 6.9 | 0.28 | 6.8 | $C_4H_{10}$ (100), $C_2H_6$ (trace) |
| | | FlTA | | |
| R = Me | | | | |
| 2.1 | 0 | 3.6 | 0 | no reaction |
| | | Fl | | |
| 3.6 | 6.9 | 3.6 | 12 | $C_2H_6$ (89), $CH_4$ (11) |
| 2.1 | 6.9 | 0 | 4.1 | $C_2H_6$ (trace), $CH_4$ (100) |
| 2.1 | 0 | 0 | 4.1 | $C_2H_6$ (trace), $CH_4$ (100) |

[a] Based on the amount of *cis*-[$R_2Co(bpy)_2$]$^+$.

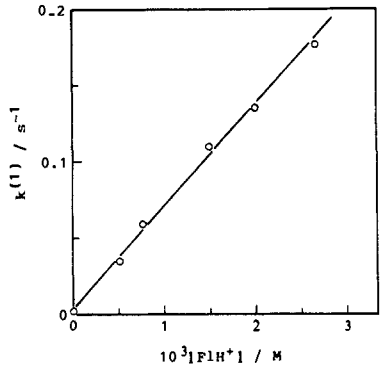


**Figure 4.** Plot of the observed pseudo-first-order rate constant $k^{(1)}$ vs the concentration of $FlH^+$ used as a catalyst for the catalytic oxidation of *cis*-[$(PhCH_2)_2Co(bpy)_2$]$^+$ by dioxygen in the presence of $HClO_4$ (0.10 M) in MeCN at 298 K.

is the main product, but a small amount of methane is also produced by the competing electrophilic cleavage of the cobalt–carbon bond with $HClO_4$.

In the absence of a coenzyme analogue, the cobalt–carbon bond of *cis*-[$Me_2Co(bpy)_2$]$^+$ in both deaerated and oxygen-saturated MeCN is cleaved by the electrophilic attack of proton to yield [$MeCo(bpy)_2$]$^{2+}$ and $CH_4$ (eq 9) (Table II).

$$cis\text{-}[Me_2Co(bpy)_2]^+ + H^+ \rightarrow CH_4 + [RCo(bpy)_2]^{2+} \quad (9)$$

**Kinetics of Coenzyme-Catalyzed Oxidation of *cis*-[$R_2Co(bpy)_2$]$^+$ with Dioxygen.** Rates of the coenzyme-catalyzed oxidation of *cis*-[$R_2Co(bpy)_2$]$^+$ by dioxygen in the presence of $HClO_4$ in MeCN obey pseudo-first-order kinetics when the concentrations of oxidants and $HClO_4$ are maintained at >10-fold excess of the concentration of *cis*-[$R_2Co(bpy)_2$]$^+$. The pseudo-first-order rate constants $k^{(1)}$ increase linearly with an increase in the concentration of a coenzyme catalyst [Cat] as shown in Figure 4. Thus, the rate of disappearance of *cis*-[$R_2Co(bpy)_2$]$^+$ is given by eq 10. The $k_{obs}$ value in air-saturated MeCN was the same as that in oxygen-saturated MeCN.

$$-d[R_2Co^+]/dt = k_{obs}[R_2Co^+][Cat] \quad (10)$$

When $FlH^+$ or $LH^+$ is used as a catalyst for the catalytic oxidation of *cis*-[$Et_2Co(bpy)_2$]$^+$ by dioxygen in the presence of $HClO_4$ in MeCN, the log $k_{obs}$ value increases linearly with an increase in the log [$HClO_4$] value with a slope of unity as shown in Figure 5. When $APH^+$ is used as a catalyst, however, the log $k_{obs}$ value remains constant with increasing [$HClO_4$] in the low-concentration region (log [$HClO_4$] < 0) and increases linearly

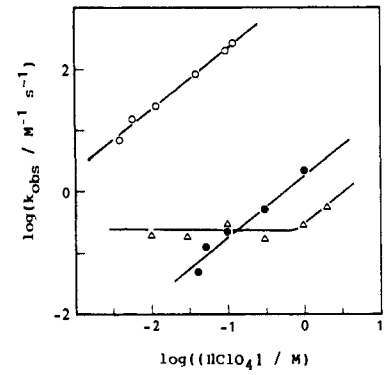


**Figure 5.** Plots of the observed second-order rate constants log $k_{obs}$ vs log [$HClO_4$] for the oxidation of *cis*-[$Et_2Co(bpy)_2$]$^+$ with dioxygen catalyzed by $FlH^+$ (○), $LH^+$ (●), and $APH^+$ (△) in the presence of $HClO_4$ in MeCN at 298 K.

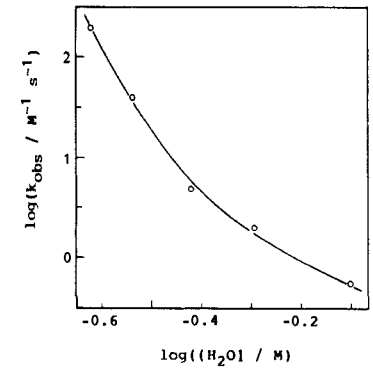


**Figure 6.** Plots of the observed second-order rate constants log $k_{obs}$ vs log [$H_2O$] for the $FlH^+$-catalyzed oxidation of *cis*-[$Et_2Co(bpy)_2$]$^+$ in the presence of $HClO_4$ (0.10 M) in MeCN containing various concentrations of $H_2O$ at 298 K.

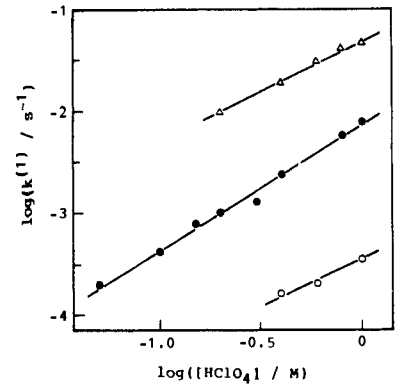


**Figure 7.** Plots of the observed pseudo-first-order rate constants log $k^{(1)}$ vs log [$HClO_4$] for the electrophilic cleavage of the cobalt–carbon bonds of *cis*-[$R_2Co(bpy)_2$]$^+$ [R = Me (△), Et (●), $PhCH_2$ (○)] by $HClO_4$ in deaerated MeCN at 298 K.

with an increase in the log [$HClO_4$] value in the higher concentration region with a slope of unity (Figure 5). The $HClO_4$ used in Figure 5 contains 30% $H_2O$ (see Experimental Section). The addition of $H_2O$ to an MeCN solution of 0.10 M $HClO_4$ results in a significant decrease in the $k_{obs}$ value as shown in Figure 6, where the log $k_{obs}$ values of the $FlH^+$-catalyzed oxidation of *cis*-[$Et_2Co(bpy)_2$]$^+$ by dioxygen are plotted against the log [$H_2O$] values.[38]

Figure 7 shows the dependence of the pseudo-first-order rate constants log $k^{(1)}$ for the electrophilic cleavage of the cobalt–carbon bonds of *cis*-[$R_2Co(bpy)_2$]$^+$ in the absence of dioxygen and coenzyme analogues on the $HClO_4$ concentration, log [$HClO_4$]. Each $k^{(1)}$ value of *cis*-[$R_2Co(bpy)_2$]$^+$ shows a first-order dependence on [$HClO_4$] and decreases in the order R = Me > Et > $PhCH_2$. Since the electrophilic cleavage of *cis*-[$R_2Co(bpy)_2$]$^+$ by $HClO_4$ is fastest for R = Me, the $k_{obs}$ values of the $FlH^+$-

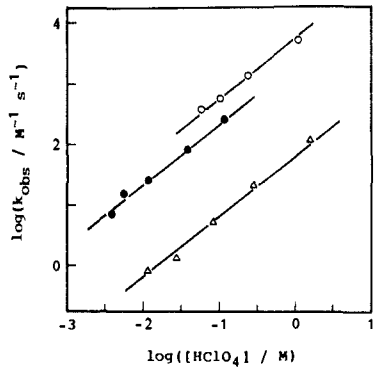


**Figure 8.** Plots of the observed second-order rate constants log $k_{obs}$ vs log [$HClO_4$] for the $FlH^+$-catalyzed oxidation of *cis*-$[R_2Co(bpy)_2]^+$ [R = $PhCH_2$ (○), Et (●), Me (△)] by dioxygen in the presence of $HClO_4$ in MeCN at 298 K.

**Table III.** Product Yields in the One-Electron Oxidation of *cis*-$[R_2Co(bpy)_2]^+$ (R = $PhCH_2$, Et, Me; 3.8 × $10^{-6}$ mol) by Various Oxidants (2.0 × $10^{-5}$ mol) in Deaerated MeCN (2.0 $cm^3$) at 298 K

| *cis*-$[R_2Co(bpy)_2]^+$ R | oxidant | products (yield,[a] %) |
|---|---|---|
| $PhCH_2$ | $[Fe(phen)_3]^{3+}$ | $PhC_2H_4Ph$ (98) |
| $PhCH_2$ | $[Fe(bpy)_3]^{3+}$ | $PhC_2H_4Ph$ (99) |
| $PhCH_2$ | DDBQ | $PhC_2H_4Ph$ (99) |
| $PhCH_2$ | DCBQ | $PhC_2H_4Ph$ (97) |
| Et | $[Fe(phen)_3]^{3+}$ | $C_4H_{10}$ (98) |
| Et | $[Fe(bpy)_3]^{3+}$ | $C_4H_{10}$ (100) |
| Et | $[Fe(C_5H_5)_2]^+$ | $C_4H_{10}$ (99) |
| Et | $[Fe(MeC_5H_4)_2]^+$ | $C_4H_{10}$ (97) |
| Et | TCNE | $C_4H_{10}$ (97) |
| Et | DDBQ | $C_4H_{10}$ (99) |
| Et | DCBQ | $C_4H_{10}$ (100) |
| Me | $[Fe(phen)_3]^{3+}$ | $C_2H_6$ (100) |
| Me | $[Fe(bpy)_3]^{3+}$ | $C_2H_6$ (100) |
| Me | DDBQ | $C_2H_6$ (100) |
| Me | DCBQ | $C_2H_6$ (100) |

[a] Based on the amount of *cis*-$[R_2Co(bpy)_2]^+$.

catalyzed reaction of *cis*-$[Me_2Co(bpy)_2]^+$ were determined under conditions such that the contribution from the electrophilic cleavage reaction by $HClO_4$ can be neglected, using a large concentration of $FlH^+$ (>1.0 × $10^{-2}$ ). Then the $k_{obs}$ values of *cis*-$[R_2Co(bpy)_2]^+$ (R = $PhCH_2$, Et, Me) are compared using the same catalyst ($FlH^+$) as shown in Figure 8, where the log $k_{obs}$ values are plotted against the log [$HClO_4$] values. The $k_{obs}$ value at the same concentration of $HClO_4$ decreases in the order R = $PhCH_2$ > Et > Me.

**Cleavage Modes of Cobalt–Carbon Bonds upon One-Electron Oxidation of *cis*-$[R_2Co(bpy)_2]^+$ in the Absence and Presence of Dioxygen.** The cleavage modes of cobalt–carbon bonds upon one-electron oxidation of *cis*-$[R_2Co^{III}(bpy)_2]^+$ are examined by determining the cleaved products in electron-transfer reactions from *cis*-$[R_2Co(bpy)_2]^+$ to strong one-electron oxidants such as $[Fe(bpy)_3]^{3+}$ and $[Fe(phen)_3]^{3+}$ in the presence and absence of dioxygen. In the absence of dioxygen, one-electron oxidation of *cis*-$[R_2Co(bpy)_2]^+$ (R = $PhCH_2$, Et, Me) yields exclusively the coupling products of the alkyl groups as shown in Table III (eq 11).[21,40] In the presence of dioxygen as well, the same coupling

$$cis\text{-}[R_2Co(bpy)_2]^+ + Ox \rightarrow R\text{-}R + [Co(bpy)_2]^{2+} + Ox^- \quad (11)$$

products are obtained in the case of R = Et and Me (Table IV). In the case of R = $PhCH_2$, however, no coupling product is obtained in the presence of dioxygen, but instead, an oxygenated product, benzaldehyde, is obtained (Table IV).

**Kinetics of One-Electron Oxidation of *cis*-$[R_2Co(bpy)_2]^+$.** Rates of electron transfer from *cis*-$[R_2Co(bpy)_2]^+$ to various one-electron oxidants (Ox), 2,3-dichloro-5,6-dicyano-*p*-benzoquinone (DDBQ), 2,3-dicyano-*p*-benzoquinone (DCBQ), tetracyanoethylene (TCNE), 7,7,8,8-tetracyano-*p*-quinodimethane (TCNQ), ferrocenium ion ($[Fe(C_5H_5)_2]^+$), *n*-butylferrocenium ion ($[Fe(BuC_5H_4)(C_5H_5)]^+$), and 1,1′-dimethylferrocenium ion $[(Fe(MeC_5H_4)_2]^+$), in deaerated MeCN obey second-order kinetics, showing a first-order dependence on the concentration of each reactant (eq 12). The observed second-order rate constants $k_{obs}$

$$d[R_2Co]/dt = -d[Ox^-]/dt = -k_{obs}[R_2Co][Ox] \quad (12)$$

are summarized in Table V, together with the one-electron redox potentials of the reactants.[21,40] The rate constant $k_{obs}$ of the same dialkylcobalt(III) complex decreases with a negative shift in the one-electron reduction potential $E^\circ_{red}$ of one-electron oxidants, when electron transfer becomes energetically less favorable (Table V). In contrast, the reactivity of *cis*-$[(PhCH_2)_2Co(bpy)_2]^+$ is surprisingly small as compared with that of the other dialkylcobalt(III) complexes *cis*-$[R_2Co(bpy)_2]^+$ (R = Et, Me), although the one-electron oxidation potential of *cis*-$[R_2Co(bpy)_2]^+$ decreases in the order R = Me > $PhCH_2$ > Et.

**Table IV.** Product Yields in the One-Electron Oxidation of *cis*-$[R_2Co(bpy)_2]^+$ (R = $PhCH_2$, Et, Me; 3.8 × $10^{-6}$ mol) by Various Oxidants (2.0 × $10^{-5}$ mol) in Oxygen-Saturated MeCN (2.0 $cm^3$) at 298 K

| *cis*-$[R_2Co(bpy)_2]^+$ R | oxidant | products (yield,[a] %) |
|---|---|---|
| $PhCH_2$ | $[Fe(phen)_3]^{3+}$ | PhCHO (99) |
| $PhCH_2$ | $[Fe(bpy)_3]^{3+}$ | PhCHO (99) |
| Et | $[Fe(phen)_3]^{3+}$ | $C_4H_{10}$ (100) |
| Et | $[Fe(bpy)_3]^{3+}$ | $C_4H_{10}$ (97) |
| Et | TCNE | $C_4H_{10}$ (96) |
| Et | DDBQ | $C_4H_{10}$ (97) |
| Et | DCBQ | $C_4H_{10}$ (100) |
| Me | $[Fe(phen)_3]^{3+}$ | $C_2H_6$ (100) |
| Me | $[Fe(bpy)_3]^{3+}$ | $C_2H_6$ (98) |
| Me | TCNE | $C_2H_6$ (94) |
| Me | DDBQ | $C_2H_6$ (99) |
| Me | DCBQ | $C_2H_6$ (100) |

[a] Based on the amount of *cis*-$[R_2Co(bpy)_2]^+$.

**Table V.** Observed Second-Order Rate Constants $k_{obs}$ for Electron-Transfer Reactions from *cis*-$[R_2Co(bpy)_2]^+$ (R = $PhCH_2$, Et, Me) to Various One-Electron Oxidants in MeCN at 298 K, the One-Electron Reduction Potentials $E^\circ_{red}$ of Oxidants, and the One-Electron Oxidation Potentials $E^\circ_{ox}$ of *cis*-$[R_2Co(bpy)_2]^+$

| | | | $k_{obs}$[a] ($M^{-1}$ $s^{-1}$) of *cis*-$[R_2Co(bpy)_2]^+$[b] | | |
|---|---|---|---|---|---|
| no. | oxidant | $E^\circ_{ox}$,[c] V | R = $PhCH_2$ (0.60 V) | R = Et (0.57 V) | R = Me (0.63 V) |
| 1 | DDBQ | 0.51 | 7.8 | $5.5 \times 10^{5}$[d] | $3.2 \times 10^{3}$[d] |
| 2 | $[Fe(C_5H_5)_2]^+$ | 0.37 | | $7.1 \times 10^{2}$ | |
| 3 | $[Fe(BuC_5H_4)(C_5H_5)]^+$ | 0.31 | | $3.3 \times 10^{2}$ | |
| 4 | DCBQ | 0.28 | $2.3 \times 10^{-3}$ | $2.3 \times 10^{2}$[d] | 1.8[d] |
| 5 | $[Fe(MeC_5H_4)_2]^+$ | 0.26 | | 4.6 × 10 | |
| 6 | TCNE | 0.22 | | $1.9 \times 10^{d}$ | $2.5 \times 10^{-1}$[d] |
| 7 | TCNQ | 0.19 | $3.5 \times 10^{-4}$ | 6.1[d] | |

[a] The experimental errors are within ±10%. [b] The $E^\circ_{ox}$ values taken from ref 21 and 40 are shown in the parentheses. [c] Taken from ref 40. [d] Taken from ref 21.

## Discussion

**Mechanism of Coenzyme-Catalyzed Oxidative Coupling of *cis*-$[R_2Co(bpy)_2]^+$ (R = Et, Me) by Dioxygen.** The formation of the coupling products of alkyl ligands of *cis*-$[R_2Co(bpy)_2]^+$ (R = Et, Me), which could only arise via the corresponding dialkylcobalt(IV) complexes, demonstrates clearly the involvement of an electron-transfer process in the coenzyme-catalyzed oxidation of *cis*-$[R_2Co(bpy)_2]^+$. The catalytic cycle in the case of $FlH^+$ is shown in Scheme I, where an acid-catalyzed electron transfer from the dialkylcobalt(III) complex ($R_2Co^+$) to $FlH^+$ occurs to give the corresponding dialkylcobalt(IV) complex ($R_2Co^{2+}$) and $FlH_2^{\bullet+}$, followed by the facile reductive elimination of the alkyl ligands to yield the coupling product R–R. The resulting cobalt(II) complex may reduce $FlH_2^{\bullet+}$ in the presence of $HClO_4$ to give $Co^{3+}$

(40) Ishikawa, K.; Fukuzumi, S.; Tanaka, T. *Inorg. Chem.* **1989**, *28*, 1661.

**Scheme I**

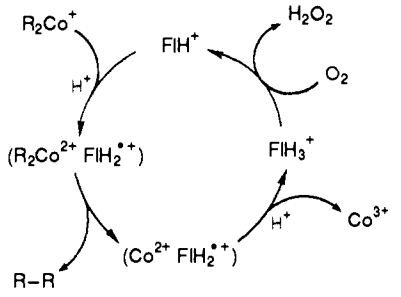


and a protonated dihydroflavin $FlH_3^+$. The fully reduced form of flavin ($FlH_3^+$) is known to be readily oxidized by dioxygen to regenerate the oxidized form ($FlH^+$) accompanied by the formation of $H_2O_2$.[18,19] In the absence of dioxygen, the dihydroflavin radical cation $FlH_2^{\bullet+}$ is formed by the comproportionation reaction (eq 13) as shown in eq 6 (Figure 2).[18,19]

$$FlH_3^+ + FlH^+ \rightleftarrows 2FlH_2^{\bullet+} \qquad (13)$$

In Scheme I, the acid-catalyzed electron transfer from $R_2Co^+$ to $FlH^+$ may be the rate-determining step, since the rate is proportional to $[R_2Co][FlH^+][H^+]$ and independent of the $O_2$ concentration (eq 10). Essentially the same reaction scheme may be applied for the $LH^+$-catalyzed oxidation of $R_2Co^+$ by dioxygen in the presence of $HClO_4$. In the case of $APH^+$, however, the rate is independent of $[HClO_4]$ in the low-concentration region ($[\log [HClO_4] < 0$) as shown in Figure 5. Such a difference may be ascribed to the difference in the acid dissociation constant ($K_a$) of $APH_2^{\bullet+}$ and $FlH_2^{\bullet+}$ (or $LH_2^{\bullet+}$) as follows. The Nernst equation for the one-electron reduction potential of $APH^+$ in the presence of $HClO_4$, $E_{red}$, may be expressed by eq 14,[33,41] where $E^\circ_{red}$ is the

$$E_{red} = E^\circ_{red} + (2.3RT/F) \log (1 + K_a^{-1}[H^+]) \qquad (14)$$

one-electron redox potential of the $APH^+/APH^\bullet$ couple, $F$ is the Faraday constant, and $2.3RT/F = 0.059$ at 298 K. According to eq 14, $E_{red}$ is independent of $[HClO_4]$ in the low-concentration region, $[HClO_4] \ll K_a$. In the higher concentration region, $[HClO_4] \gg K_a$, the reduced form of $APH^+$ may exist predominantly as $APH_2^{\bullet+}$, when the $E_{red}$ value is shifted to the positive direction with an increase in the $HClO_4$ concentration and thus, the one-electron reduction of $APH^+$ becomes energetically more favorable. If the activation Gibbs free energy change $\Delta G^\ddagger_{et}$ of electron transfer is directly related with the corresponding standard Gibbs free energy change, i.e., $\Delta G^\ddagger_{et} \cong \Delta G^\circ_{et} = F(E^\circ_{ox} - E^\circ_{red})$, from eq 14 is derived the dependence of the rate constant $k_{et}$ of electron transfer on $[HClO_4]$, as shown in eq 15, where $C$ is a

$$\log k_{et} = \log (1 + K_a^{-1}[H^+]) + C \qquad (15)$$

constant.[42] Equation 15 agrees well with the experimental results in Figure 5, where the observed rate constant $k_{obs}$, which may be equal to $k_{et}$ of the rate-limiting electron-transfer step in eq 15, is independent of $[HClO_4]$ in the low-concentration region ($\log [HClO_4] < 0$) but $k_{obs}$ increases showing a first-order dependence on $[HClO_4]$ in the higher concentration region. Thus, the $\log K_a$ value of $APH_2^{\bullet+}$ is obtained as ca. 0 from the dependence of $k_{obs}$ on $[HClO_4]$. In the case of $FlH^+$ and $LH^+$, the $\log K_a$ values of $FlH_2^{\bullet+}$ and $LH_2^{\bullet+}$ may be smaller than ca. −3 and −2, respectively. This may be the reason why $FlH_2^{\bullet+}$ and $LH_2^{\bullet+}$ radical cations are observed in electron-transfer reactions from *cis*-$[Et_2Co(bpy)_2]^+$ to $FlH^+$ and $LH^+$ in the presence of $HClO_4$ ($1.0 \times 10^{-2}$ M) in deaerated MeCN but $APH_2^{\bullet+}$ radical cation is not observed (vide supra).

**Mechanism of Catalytic Oxygenation of the Benzyl Ligand of *cis*-$[(PhCH_2)_2Co(bpy)_2]^+$.** The product in the coenzyme-catalyzed oxidation of *cis*-$[R_2Co(bpy)_2]^+$ by dioxygen in the case of R = $PhCH_2$ is drastically changed from R–R in the case of R = Et or Me (Table II) to the oxygenated product PhCHO (Table I). Such a change in the products depending on the alkyl ligands is also observed in the one-electron oxidation of *cis*-$[R_2Co(bpy)_2]^+$ in the presence of dioxygen (Table IV). In order to elucidate the origin of such a difference, we discuss hereafter the difference in the reactivities of *cis*-$[R_2Co(bpy)_2]^+$ in the electron-transfer reactions.

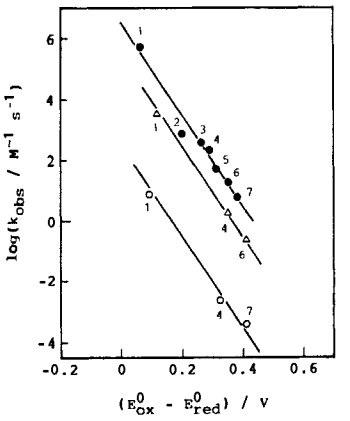


**Figure 9.** Plots of $\log k_{obs}$ for electron-transfer reactions from *cis*-$[R_2Co(bpy)_2]^+$ [R = $PhCH_2$ (○), Et (●), Me (△)] to oxidants vs the difference in the redox potentials between $E^\circ_{ox}$ of *cis*-$[R_2Co(bpy)_2]^+$ and $E^\circ_{red}$ of the oxidants. Numbers refer to the oxidants in Table V.

**Scheme II**

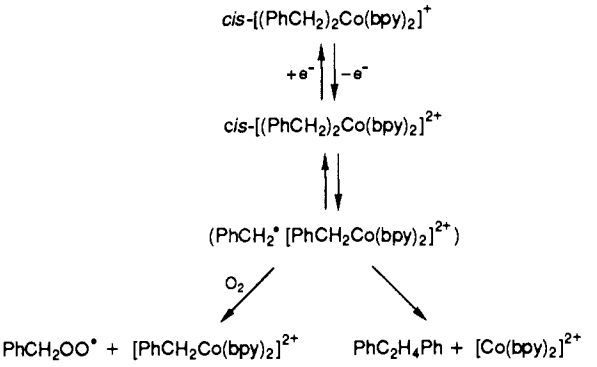


The $\log k_{obs}$ values in Table V are plotted against the difference in the redox potentials of *cis*-$[R_2Co(bpy)_2]^+$ and the oxidant, $E^\circ_{ox} - E^\circ_{red}$, which corresponds to the Gibbs free energy change of electron transfer $\Delta G^\circ_{et}$, as shown in Figure 9. For each *cis*-$[R_2Co(bpy)_2]^+$ a linear correlation is observed between $\log k_{obs}$ and $E^\circ_{ox} - E^\circ_{red}$. Each slope is about the same, ca. −15, which corresponds to $-F/(2.3RT)$ at 298 K. Thus, the decrease in the $\Delta G^\circ_{et}$ value [$=F(E^\circ_{ox} - E^\circ_{red})$] with an increase in the $E^\circ_{red}$ value of various oxidants is directly reflected in the increase in the rate constant [$\log k_{obs} = \log Z - \Delta G^\ddagger_{et}/(2.3RT)$].[43] The $k_{obs}$ value of *cis*-$[R_2Co(bpy)_2]^+$ at the same $E^\circ_{ox} - E^\circ_{red}$ value is in the order R = Et = Me ≫ $PhCH_2$ (Figure 9). The low reactivity of *cis*-$[(PhCH_2)_2Co(bpy)_2]^+$, together with formation of the oxygenated product instead of the coupling product upon the one-electron oxidation in the presence of dioxygen, suggests that the cleavage of cobalt–benzyl bond of *cis*-$[(PhCH_2)_2Co(bpy)_2]^{2+}$ occurs in a stepwise manner and that the benzyl radical formed is stable enough to be trapped by dioxygen to give benzylperoxy radical as shown in Scheme II. The rates of reactions of alkyl radicals (Me•, Et•, and $PhCH_2^\bullet$) with a dioxygen to produce alkylperoxy radicals are known to be close to the diffusion-controlled limit.[44] The benzylperoxy radical may decay by the bimolecular reaction to yield benzaldehyde and benzyl alcohol,[14a,45]

(41) Meites, L. *Polarographic Techniques*, 2nd ed.; Wiley: New York, 1965; pp 203–301.

(42) The constant $C$ is equal to $\log Z - F(E^\circ_{ox} - E^\circ_{red})/(2.3RT)$, in which $Z$ is the frequency factor, taken as $10^{11}$ $M^{-1}$ $s^{-1}$.

(43) If the activation Gibbs free energy $\Delta G^\ddagger_{et}$ is proportional to $\Delta G^\circ_{et}$, $k_{obs}$ may be given by $k_{obs}$ = constant + $F(E^\circ_{ox} - E^\circ_{red})/(2.3RT)$, in which the slope of the plot of $\log k_{obs}$ vs $E^\circ_{ox} - E^\circ_{red}$ would be equal to $-F/(2.3RT) = -16.9$ at 298 K.[21]

(44) Howard, J. A. *Free Radicals*; Kochi, J. K., Ed.; Wiley: New York, 1973; Vol. II, p 3.

**Scheme III**

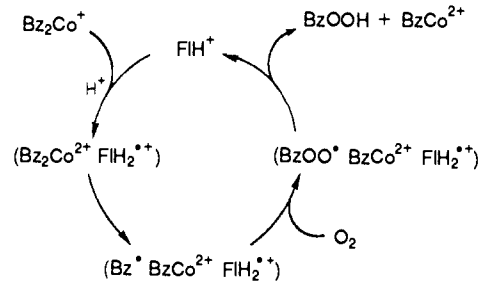


the latter of which may be further oxidized by the oxidant to give benzaldehyde as the final oxygenated product (Table IV). In the absence of dioxygen, the benzyl radical may react with $[PhCH_2Co(bpy)_2]^{2+}$ in the cage to yield the coupling product, $PhC_2H_2Ph$ (Table III). In the case of *cis*-$[R_2Co(bpy)_2]^+$ (R = Et, Me) as well, the cleavage of the Co–R bond upon the one-electron oxidation may occur in a stepwise manner as shown in Scheme II. However, rates of the reactions of much more reactive radicals R• (Et• or Me•) with $[RCo(bpy)_2]^{2+}$ as compared to benzyl radicals may be so fast that R• radicals cannot be trapped by dioxygen and that only the net coupling of the alkyl ligands of $[R_2Co(bpy)_2]^{2+}$ can occur to yield the coupling products R–R exclusively. Such higher reactivities of ethyl and methyl radicals as compared to benzyl radical are known in the reactions with various thiols.[46]

On the basis of the above discussion, the catalytic cycle for the coenzyme-catalyzed oxygenation of the benzyl ligand of *cis*-$[(PhCH_2)_2Co(bpy)_2]^+$ ($Bz_2Co^+$) in the case of $FlH^+$ may be shown in Scheme III. At first, an acid-catalyzed electron transfer from $Bz_2Co^+$ to $FlH^+$ occurs to give ($Bz_2Co^{2+}$ $FlH_2^{\bullet+}$). One cobalt–benzyl bond in $Bz_2Co^{2+}$ may be readily cleaved to give benzyl radical (Bz•), followed by the facile trap by dioxygen to produce benzylperoxy radical (BzOO•), which then gives benzyl hydroperoxide (BzOOH) by the abstraction of hydrogen atom from $FlH_2^{\bullet+}$, accompanied by regeneration of $FlH^+$. The benzyl hydroperoxide may decompose to give the final product, benzaldehyde.[31] Essentially the same reaction scheme may be applied for the case of $LH^+$. In the case of $APH^+$, however, the initial electron transfer from $Bz_2Co^+$ to $APH^+$ produces APH• instead of $APH_2^{\bullet+}$ as indicated by the dependence of log $k_{obs}$ on $[HClO_4]$ (Figure 5).

Comparison of Schemes I and III reveals the origin of the difference in the oxygenation and oxidative coupling processes, that is, the much lower reactivity of benzyl radicals as compared to methyl or ethyl radicals in the coupling reactions, resulting in the trapping of benzyl radical by dioxygen to lead to the oxygenated product, benzyl hydroperoxide. As such, *cis*-$[(PhCH_2)_2Co(bpy)_2]^+$ is the least reactive in the one-electron oxidation in the absence of dioxygen because of the slow coupling process in Scheme II (Figure 9), but it becomes the most reactive in the coenzyme-catalyzed reaction in the presence of dioxygen in Scheme III because of the facile trapping of benzyl radical by dioxygen (Figure 8).

**Acknowledgment.** This work was supported in part by a Grant-in-Aid (to S.F.) for Scientific Research from the Ministry of Education, Science and Culture, Japan.

**Registry No.** *cis*-$[(PhCH_2)_2Co(bpy)_2]ClO_4$, 104013-22-1; *cis*-$[Et_2Co(bpy)_2]ClO_4$, 91731-09-8; *cis*-$[Me_2Co(bpy)_2]ClO_4$, 91731-08-7; $HClO_4$, 7601-90-3; riboflavin-2′,3′,4′,5′-tetraacetate, 752-13-6; riboflavin, 83-88-5; lumazine, 487-21-8; aminopterin, 54-62-6.

(45) Maillard, B.; Ingold, K. U.; Scaiano, J. C. *J. Am. Chem. Soc.* **1983**, *105*, 5095.
(46) Burkhart, R. D. *J. Phys. Chem.* **1969**, *73*, 2703.

# New Niobium Complexes with Alkynes. 2. Tetranuclear Compounds with Nb–Nb Bonds, an Unprecedented Type of Tetracarbon Ligand, and Oxygen in a Rectangular Environment

**F. Albert Cotton* and Maoyu Shang**

*Contribution from the Department of Chemistry and Laboratory for Molecular Structure and Bonding, Texas A&M University, College Station, Texas 77843.* *Received July 3, 1989*

**Abstract:** Three compounds containing the tetranuclear anion $[Nb_4OCl_8\{(PhC)_4\}_2]^{2-}$ have been prepared by (**1**) reduction of $NbCl_4(THF)_2$ with Mg in the presence of PhCCPh, (**2**) by reduction of $NbCl_3(PhCCPh)(THF)_2$ with Na/Hg, and (**3**) by reduction of $NbCl_3(PhCCPh)(THF)_2$ with Na/Hg in the presence of $PEt_3$. The anion consists of a planar, rectangular $Nb_4$ group (Nb–Nb = 2.605 (3) and 3.340 (3) Å) with an oxygen atom at the center (mean Nb–O = 2.118 (1) Å). The long Nb···Nb edges are doubly bridged by Cl atoms, and there is one terminal Cl atom on each Nb atom. A C-shaped PhC–C(Ph)C(Ph)–CPh chain clasps each short Nb–Nb edge at the middle and lies in a plane perpendicular to the $Nb_4O$ plane. This $C_4$ chain and its mode of bonding to the pair of metal atoms has all C–C distances essentially equal at ca. 1.458 (9) Å. The four Nb–C distances to terminal C atoms have an average value of 2.133 (16) Å, and the four Nb–C distances to inner C atoms have an average value of 2.361 (5) Å. Crystallographic data for the three compounds are as follows: (**1**) $[Mg_2Cl_3(THF)_6]_2[Nb_4OCl_8\{(PhC)_4\}_2]\cdot 6THF$, space group $P\bar{1}$, $a$ = 15.200 (3) Å, $b$ = 15.515 (4) Å, $c$ = 16.306 (3) Å, $\alpha$ = 98.93 (2)°, $\beta$ = 106.90 (2)°, $\gamma$ = 102.97 (2)°, $V$ = 3484 (3) Å$^3$, $Z$ = 1; (**2**) $Na_2[Nb_4OCl_8\{(PhC)_4\}_2]\cdot(THF)_6(C_6H_6)_2$, space group $P\bar{1}$, $a$ = 11.802 (3) Å, $b$ = 17.311 (2) Å, $c$ = 22.966 (4) Å, $\alpha$ = 98.91 (1)°, $\beta$ = 91.61 (1)°, $\gamma$ = 103.55 (1)°, $V$ = 4496 (3) Å, $Z$ = 2; (**3**) $(HPEt_3)_2[Nb_4OCl_8\{(PhC)_4\}_2]\cdot 2C_6H_6$, space group $P\bar{1}$, $a$ = 12.831 (1) Å, $b$ = 13.194 (1) Å, $c$ = 14.219 (1) Å, $\alpha$ = 68.040 (8)°, $\beta$ = 66.616 (7)°, $\gamma$ = 66.704 (7)°, $V$ = 1961.0 (4) Å$^3$, $Z$ = 1.

There have been previous reports of the formation of alkyne complexes of niobium and tantalum.[1-3] Most of these compounds have discrete RCCR groups strongly bound to the metal atom, with M–C distances in the range 2.03–2.07 Å, and it has been

0002-7863/90/1512-1584$02.50/0 